11

Hot Spots and Mantle Plumes

11.1 Introduction

Hot spots are anomalous areas of surface volcanism that cannot be directly associated with plate tectonic processes. The term hot spot is used rather loosely. It is often applied to any long-lived volcanic center that is not part of the global network of mid-ocean ridges and island arcs. The classic example is Hawaii. Anomalous regions of thick crust on ocean ridges are also considered to be hot spots. The prototype example is Iceland.

There is little agreement on the total number of hot spots. Several hot spot lists have been published, and the number of volcanic centers included on these lists ranges from about 20 to more than 100. In one of his original papers associating hot spots with mantle plumes, Morgan (1972) listed 19 hot spots. Crough and Jurdy (1980) listed 42, Wilson (1973) listed 66, and Vogt (1981) listed 117. Table 11.1 gives the coordinates of 30 hot spots from the list of Crough and Jurdy (1980), and Figure 11.1 shows the locations of 20 prominent hot spots (see also Figure 2.23). In many cases hot spots have well-defined tracks associated with volcanic ridges or lines of volcanic edifices; these are also shown in Figure 11.1 and in Figure 2.23. A few hot spots and the tracks they have made appear on all lists, either because of high eruption rates in the recent past or because they have produced conspicuous traces. Among these are Hawaii, Iceland, Reunion, Cape Verde, and the Azores. Others, such as Bermuda, do not have an extensive volcanic history, but qualify as hot spots because they sit atop broad topographic rises or seafloor swells. Large continental volcanic centers, such as Yellowstone and some in East Africa, make most lists because of their similarity to oceanic hot spots.

The concept of stationary heat sources in the mantle was introduced by Wilson (1963c) as an explanation for the Hawaiian chain. Morgan (1971, 1972) was the first to advocate a global array of deep mantle plumes for the origin of hot spots. Morgan envisioned mantle plumes to be vertical conduits in which hot mantle material rises buoyantly from the lower mantle to the lithosphere at velocities as large as $1 \, \text{m} \, \text{yr}^{-1}$. The plume concept has steadily gained acceptance in spite of the fact that the geological, geophysical, and geochemical evidence for plumes, while growing, is still largely indirect. There are also some critical observations that plume theory has never satisfactorily explained.

Table 11.1. *Hot Spot Locations[a]*

Hot Spot	Overlying Plate	Latitude (degree)	Longitude (degree)
Hawaii	Pacific	20	−157
Samoa	Pacific	−13	−173
St. Helena	Africa	−14	−6
Bermuda	N. America	33	−67
Cape Verde	Africa	14	−20
Pitcairn	Pacific	−26	−132
MacDonald	Pacific	−30	−140
Marquesas	Pacific	−10	−138
Tahiti	Pacific	−17	−151
Easter	Pac-Naz	−27	−110
Reunion	Indian	−20	55
Yellowstone	N. America	43	−111
Galapagos	Nazca	0	−92
Juan Fernandez	Nazca	−34	−83
Ethiopia	Africa	8	37
Ascencion	S. Am-Afr	−8	−14
Afar	Africa	10	43
Azores	Eurasia	39	−28
Iceland	N. Am-Eur	65	−20
Madeira	Africa	32	−18
Canary	Africa	28	−17
Hoggar	Ind-Ant	−49	69
Bouvet	Afr-Ant	−54	2
Pr. Edward	Afr-Ant	−45	50
Eifel	Eurasia	48	8
San Felix	Nazca	−24	−82
Tibesti	Africa	18	22
Trinadade	S. America	−20	−30
Tristan	S. Am-Afr	−36	−13

[a] After Crough and Jurdy (1980).

***Question 11.1:** Do mantle plumes exist?*

***Question 11.2:** Which "hot spots" are associated with mantle plumes?*

Although the direct evidence (e.g., Wolfe et al., 1997) for the existence of mantle plumes is sparse, their occurrence is consistent with our present understanding of mantle dynamics. We routinely associate the subducted lithosphere with the instability of the upper thermal boundary layer. We also expect a thermal boundary layer at the base of the convecting layer, the D'' layer at the bottom of the mantle or an internal thermal boundary layer for layered mantle convection. Instabilities of this basal thermal boundary layer would be expected to generate mantle plumes.
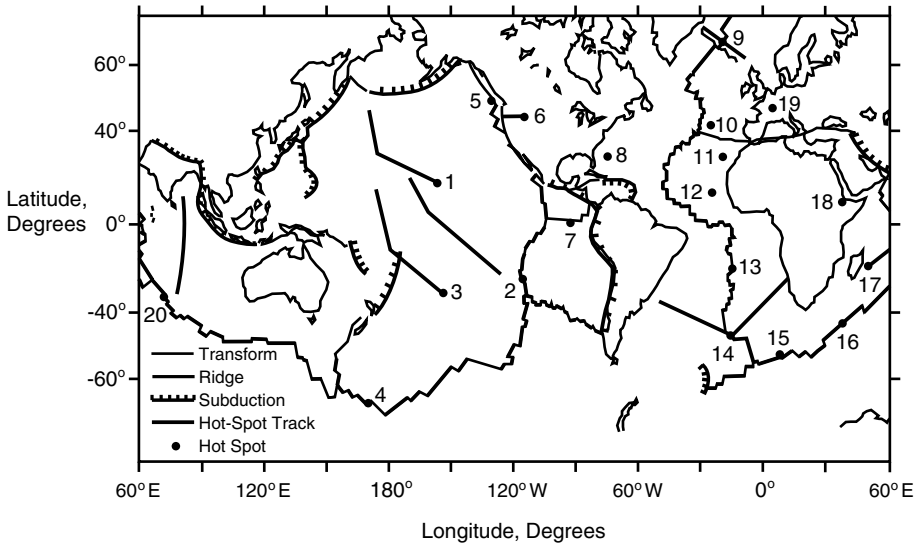
Figure 11.1. Hot spot and hot spot track locations: 1, Hawaii (Hawaiian-Emperor Seamount Chain); 2, Easter (Tuomoto-Line Island Chain); 3, MacDonald Seamount (Austral-Gilbert-Marshall Island Chain); 4, Bellany Island; 5, Cobb Seamount (Juan de Fuca Ridge); 6, Yellowstone (Snake River Plain-Columbia Plateau); 7, Galapagos Islands; 8, Bermuda; 9, Iceland; 10, Azores; 11, Canary Islands; 12, Cape Verde Islands; 13, St. Helena; 14, Tristan da Cunha (Rio Grande Ridge (w), Walvis Ridge (e)); 15, Bouvet Island; 16, Prince Edward Island; 17, Reunion Island (Mauritius Plateau, Chagos-Lacadive Ridge); 18, Afar; 19, Eifel; 20, Kerguelen Plateau (Ninety-East Ridge).

11.2   Hot Spot Tracks

The prototype of a hot spot track is the Hawaiian-Emperor chain of volcanic islands and seamounts (see Figure 2.24). The associated hot spot volcanism has resulted in a nearly continuous volcanic ridge that extends some 4,000 km from near the Aleutian Islands to the now very active Kilauea volcano on the big island of Hawaii, as illustrated in Figure 11.2a. The chain is composed of more than 100 individual volcanic shields. There is a remarkably uniform age progression, with the age of each volcanic shield increasing nearly linearly with distance from Kilauea. The average propagation rate of the track across the Pacific plate has been about 90 mm yr^{-1} over the past 40 Myr and the average time interval between formation of successive shields is about 0.7 Myr. This age progression is illustrated in Figure 11.2c.

A striking feature of this track is the bend that separates the near-linear track of the Emperor chain from the near-linear track of the Hawaiian chain. The bend in the track occurred at about 43 Myr ago when there was an abrupt shift in the position of the pole of rotation of the Pacific plate. This shift was part of a global reorientation of plate motions over a span of a few million years (Richards and Lithgow-Bertelloni, 1996) and has been associated with the continental collision between India and Asia. The rate of volcanism associated with the Hawaiian-Emperor chain has been variable, as illustrated in Figure 11.2d. Following the bend, volcanic activity was low for about 10 Myr; since then activity has generally increased with time.

Many hot spots are associated with linear tracks, as indicated in Figure 11.1. When the relative motions of the plates are removed, the hot spots appear to move together. This behavior led Morgan (1972) to conclude that hot spots are fixed with respect to the mantle.

Numerous analyses of hot spot track and plate motion directions have established that hot spots are indeed relatively stationary for time intervals of 50–100 Myr (Morgan, 1983; Jurdy and Gordon, 1984). However, they are certainly not precisely fixed. Their motion is, nevertheless, significantly slower than seafloor spreading rates. For example, Molnar and Atwater (1973) and Molnar and Stock (1987) detect relative motion between Hawaii and hot spots in the Atlantic and Indian Oceans amounting to a few mm yr^{-1}. A more recent study of hot spot fixity by Steinberger and O'Connell (1998) calculated the hot spot motion expected from the advection of mantle plumes by large-scale flow in the mantle driven by a combination of surface plate motions and lower mantle density heterogeneity, and found relative velocity between hot spots up to 10 mm yr^{-1}. It is important to emphasize that this relative stationarity is not an accurate description of every hot spot. Many hot spots are variable, and these produce either segmented tracks or, in some cases, a short pulse of activity. Other hot spots have simultaneously active volcanism at several places along the track. For these, the concept of approximate stationarity is less meaningful. Even the Hawaiian hot spot, which has persisted for 110 Myr, has exhibited large variations in its strength, as evidenced by variations in the rates of melt production and swell formation (Davies, 1992).
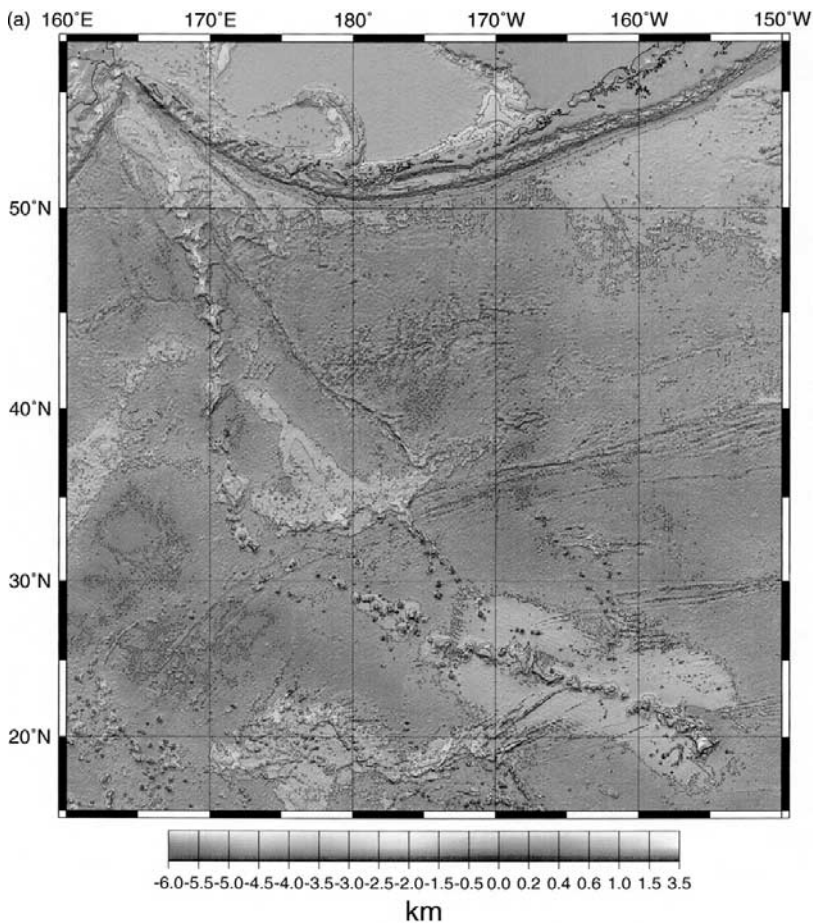

Figure 11.2. (a) Seafloor topography in the region around the Hawaiian-Emperor chain, after Smith and Sandwell (1997). (Continued)

Figure 11.2. (b) Volcanic centers in the Hawaiian-Emperor chain, from Bargar and Jackson (1974). (Continued)
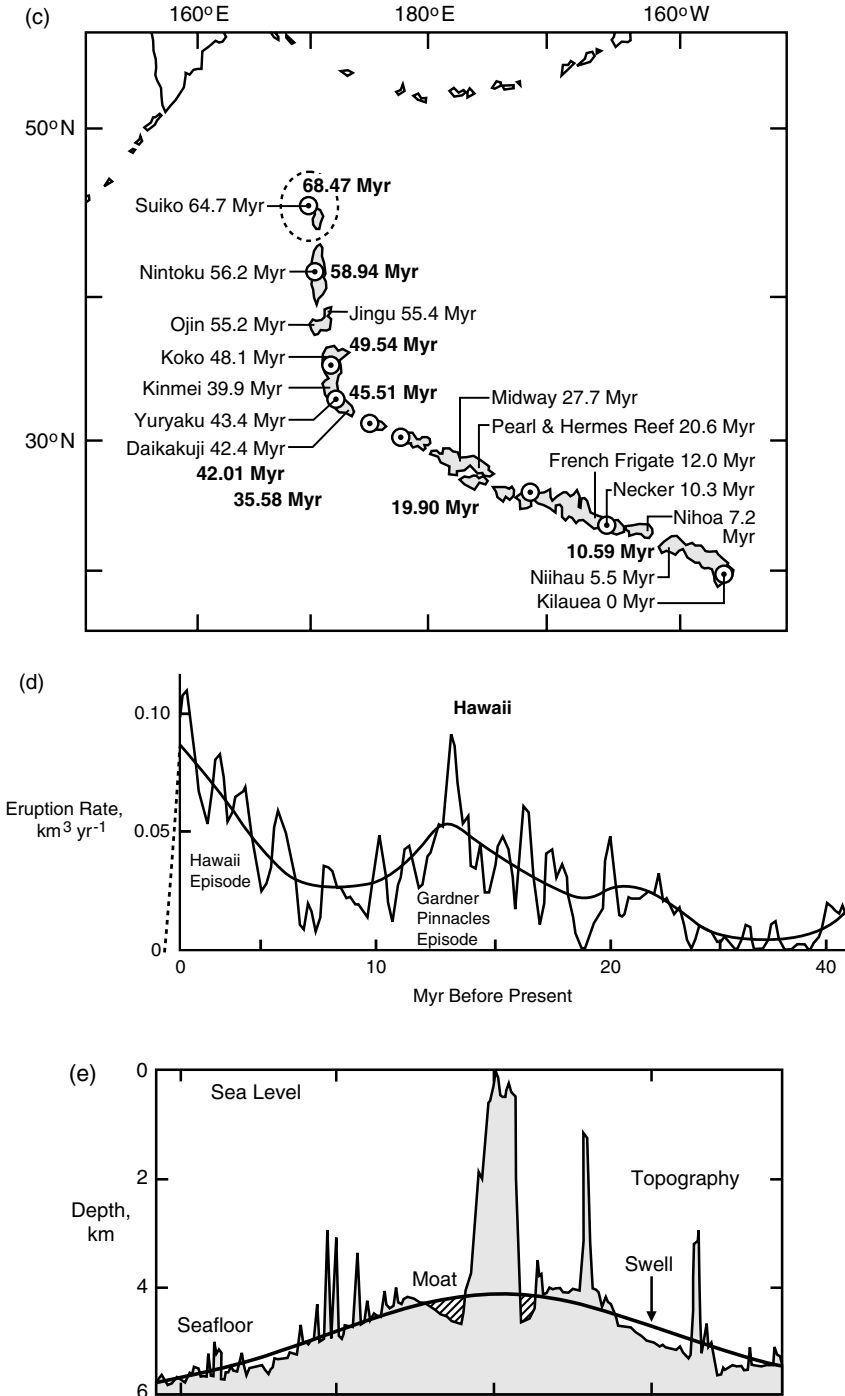
503

Figure 11.2. (c) Age progression along the chain, from Molnar and Stock (1987). (d) Estimated eruption rates versus time along the chain, from Vogt (1979). (e) Bathymetric and gravity profiles across the Hawaiian ridge at Oahu, from Watts (1976).

At the time of going to press a colour version of this figure was available for download from
http://www.cambridge.org/**9780521798365**

Hot spots appear to be better defined in the ocean basins than in the continents. Certainly not all the volcanism of the western United States can be associated with a series of hot spots. The volcanism at Yellowstone with the associated track along the Snake River Plain appears to fit most definitions of a hot spot. But other volcanism in the western United States is probably due to a thin weak lithosphere and a near surface source rather than deep-seated plumes.

11.3 Hot Spot Swells

Most hot spots are associated with topographic swells. Hot spot swells are regional topographic highs with widths of about 1,000 km and up to 3 km of anomalous elevation. The swell associated with the Hawaiian hot spot is illustrated in Figure 11.2e. The swell is roughly parabolic in planform and it extends upstream of the active hot spot, i.e., toward the spreading center of the East Pacific Rise. The excess elevation associated with the swell decays rather slowly down the track of the hot spot.

There is considerable observational evidence that the topography of hot spot swells is directly associated with a geoid anomaly (Haxby and Turcotte, 1978). This correspondence is strong evidence that the excess topography and mass of the swell are compensated at depth by anomalously light, possibly hot mantle rock. One model for isostatic compensation assumes horizontal variations in density over a prescribed depth W, the so-called Pratt compensation. The variable density ρ_p is related to the elevation h above the adjacent ocean basins by

$$\rho_p = \frac{\rho_0 W + \rho_w h}{W + h} \tag{11.3.1}$$

where ρ_0 is the reference density corresponding to zero elevation, ρ_w is seawater density, and W is referred to as the depth of compensation. With the ocean basin as reference, the geoid anomaly ΔN associated with the compensated topography is

$$\Delta N = -\frac{2\pi G}{g} \left[\int_{-h}^0 \left(\rho_p - \rho_w\right) y \, dy + \int_0^W \left(\rho_p - \rho_0\right) y \, dy \right] = \frac{\pi G \left(\rho_0 - \rho_w\right)}{g} hW \tag{11.3.2}$$

The geoid anomaly is linearly dependent on the topography so that the local geoid to topography ratio GTR should be a constant for each swell.

The dependence of the observed geoid anomalies on bathymetry across the Hawaiian and Bermuda swells is given in Figure 11.3. Also included are the predicted geoid anomalies from (11.3.2) for $\rho_0 = 3{,}300 \, \text{kg m}^{-3}$, $\rho_w = 1{,}000 \, \text{kg m}^{-3}$, and several values of W. Within the scatter of the data, good agreement is obtained for Pratt compensation with a depth of compensation W of about 100 km. Geoid topography ratios for a variety of oceanic swells have been compiled by Sandwell and MacKenzie (1989). Their results are given in Figure 11.4. It is significant that none of the hot spot geoid anomalies shows evidence of very deep compensation.

The cause of hot spot swells and how the topography is compensated remain subjects of some controversy (Sleep, 1992). Several theories have been proposed for the origin of hot spot swells. Crough (1978, 1983) and Detrick and Crough (1978) proposed a thermal rejuvenation hypothesis associated with a thinning of the lithosphere. They proposed that the flow associated with an impinging plume thinned the thermal lithosphere in the vicinity of the active hot spot and supported this argument by comparing the decay of the swell downstream
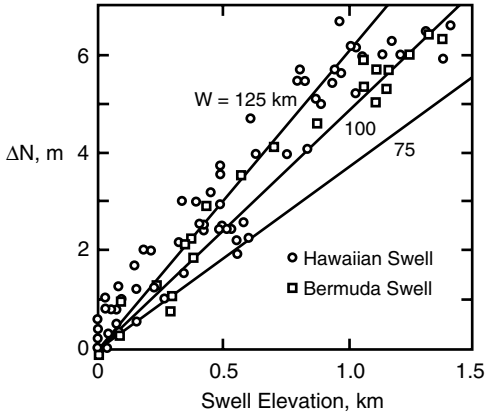
Figure 11.3. Dependence of the observed geoid anomalies ΔN on bathymetry across the Hawaiian and Bermuda Swells (Crough, 1978; Haxby and Turcotte, 1978) compared with the theoretical prediction (11.3.2) of Pratt compensation models with various depths of compensation W.
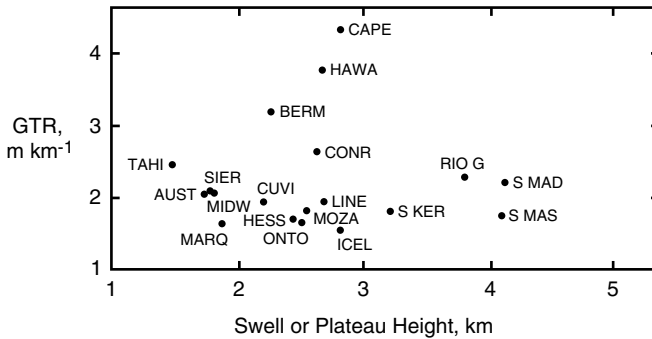

Figure 11.4. Dependence of the geoid to topography ratio (GTR) on maximum topography for various oceanic swells (Sandwell and MacKenzie, 1989). Cape Verde Rise (CAPE), Hawaiian Swell (HAWA), Bermuda Swell (BERM), Conrad Rise (CONR), Tahiti Swell (TAHI), Austral Swell (AUST), Sierra Leone Rise (SIER), Midway Swell (MIDW), Marquesas Swell (MARQ), Cuvrer and Wallaby Plateaus (CUVI), Hess Rise (HESS), Ontong-Java Plateau (ONTO), Mozambique Plateau (MOZA), Line Swell (LINE), Iceland (ICEL), South Kerguelen Plateau (S KER), Rio Grande Rise (RIO G), South Mascarene Plateau (S MAS), South Madagascar Ridge (S MAD).

of the Hawaiian hot spot with the cooling of a reheated lithospheric plate. Related numerical calculations have also been carried out by Sandwell (1982), Sleep (1987), and Liu and Chase (1989). Moore and Schubert (1997a) argue that the sign of the curvature of the observed geoid–topography relation favors the lithospheric thinning hypothesis.

Nevertheless, there are a number of uncertainties with lithospheric thinning as the cause of hot spot swells. On one hand, Emerman and Turcotte (1983), Monnereau et al. (1993), and Davies (1994) argued that thermal erosion by a plume is an inefficient means of thinning the lithosphere. Their thermomechanical models produced rates of thinning that are about an order of magnitude too slow to provide thermal rejuvenation. On the other hand, more recent, fully three dimensional numerical calculations of plume–lithosphere interactions incorporating strongly temperature-dependent viscosity show that the impingement of plumes at the base of the lithosphere leads to gravitational instability and sinking of parts of the lower lithosphere above the plume, a process that rapidly thins the lithosphere (Moore et al., 1998b, 1999).

A second argument against the lithospheric thinning hypothesis comes from heat flow measurements along hot spot tracks. If hot spots erode the lithosphere and reset the thickness of the plate to a value appropriate to a younger age, then greater heat flow and rate of subsidence would be observed, as compared to undisturbed lithosphere with the same age (Crough, 1978). From the cooling half-space model presented in Chapter 4, the relationship between rate of subsidence of the swell $d(h_\infty - h)/dt$ and anomalous surface heat flow $q - q_\infty$ is

$$\frac{d(h_\infty - h)}{dt} = \frac{\alpha(q - q_\infty)}{c_p(\rho_m - \rho_w)} \tag{11.3.3}$$

where α is thermal expansivity, $\rho_m - \rho_w$ is the mantle–seawater density contrast, c_p is specific heat, and the subscript ∞ refers to values on the seafloor far from the swell. Small heat flow anomalies, of about 5–$10\,\mathrm{mW\,m^{-2}}$, have been measured on the flanks of some oceanic hot spot swells (Detrick et al., 1981, 1986; Von Herzen et al., 1982; Bonneville et al., 1997). However, heat flow determinations by Von Herzen et al. (1989) indicate that the excess oceanic heat flow over the Hawaiian swell is too small by nearly an order of magnitude for consistency with the thinned lithosphere required to produce the observed swell topography, according to (11.3.3). Of course, the lithosphere could be thinned at a hot spot swell before a new steady conductive thermal state is established in the thinner lithosphere. In this event, an excess heat flow would not be measured at the surface above the swell.

A second class of models for hot spot swells involves dynamic support by viscous plume flow without any lithosphere thinning. When the hot plume flow reaches the base of the lithosphere it must flow radially outward along the bottom of the lithosphere. A mushroom-shaped cap forms at the top of the plume as it is deflected by the lithosphere (Olson et al., 1988) (see Figure 11.18a). The result of the lateral plume deflection is a horizontal pressure gradient with the highest pressure at the center of the plume. This pressure results in uplift of the lithosphere and a hot spot swell.

Another source of support for hot spot swells is the buoyancy of the hot plume material in the asthenosphere. The anomalously hot plume material that spreads out beneath the lithosphere has a thermal buoyancy that can produce uplift. Beneath a moving plate, the plume cap is advected in the direction of plate motion and spreads by viscous flow in the transverse direction, as shown in three-dimensional plume calculations (Ribe and Christensen, 1994; Moore et al., 1998b). This effect, coupled with the time variability in source strength at hot spots (Davies, 1992), can explain the evolution of hot spot swells without the need to invoke lithospheric thinning. Based on a series of numerical calculations, Robinson et al. (1987) and Robinson and Parsons (1988) have argued that a low viscosity asthenosphere beneath a swell can give geoid–topography correlations for dynamic support that are indistinguishable from those of lithospheric thinning models.

A variation on the thermal buoyancy model has been proposed by Phipps Morgan et al. (1995), who argue that compositional buoyancy associated with depleted mantle rock is responsible for the uplift of a hot spot swell. However, Moore and Schubert (1997a) showed that the sign of the curvature in the observed geoid–topography relation for the Hawaiian swell is opposite to what would be expected for chemical compositional buoyancy.

Question 11.3: *What mechanism is responsible for the formation of hot spot swells?*

11.4   Hot Spot Basalts and Excess Temperature

A large fraction of the volcanic rocks associated with hot spots have a basaltic composition with a major element chemistry very similar to that of mid-ocean ridge basalt (MORB). However, there are significant differences in both trace element composition and isotope ratios. These differences are discussed in detail in Chapter 12.

Whereas MORB forms by partial melting of mantle peridotites previously depleted in incompatible trace elements such as K, Rb, U, and Th, ocean island basalt (OIB) produced at hot spots often lacks this depletion in trace elements, indicating that OIB comes from a distinct parent material. Isotopic compositions indicate that OIB is derived from a mixture of sources, including the depleted MORB source, possibly a more primitive mantle component, and one or more enriched sources (possibly recycled continental crust or subcontinental lithosphere).

MORB is a result of pressure-release melting within large-scale upwellings beneath actively spreading ridges. As discussed in Chapter 3, seismic evidence indicates that these upwellings generally do not extend through the transition zone, and in many cases may be even shallower. If this is true, then most of the material in the upwellings beneath spreading centers comes from the upper mantle.

In contrast, there are various lines of evidence indicating that the source for hot spots lies deeper in the mantle and is associated with upwellings that are several hundred degrees hotter than beneath normal spreading centers. Ridge-centered hot spots such as Iceland produce much thicker crust than do the ridges on which they lie (White, 1993). We have shown in Chapter 4 that the amount of basalt melt produced in an upwelling depends primarily on the depth at which the rising material intersects the solidus, which in turn depends on the potential (zero pressure) temperature of the adiabat on which the ascending material lies. Greater crustal thickness at ridge-centered hot spots indicates higher mantle temperatures at the hot spot, compared with other parts of the ridge. The calculations of pressure-release partial melting in Chapter 4 indicate that the extra crustal thickness at hot spots requires the temperature in hot spot upwellings to be 200–300 K above the potential temperature (1,600 K) of a normal mantle adiabat. Because subsolidus upwellings in the mantle are nearly isentropic, the excess temperature beneath hot spots must be derived from a region of the mantle with higher potential temperature than the normal upper mantle which forms the ridges. The higher upwelling temperatures therefore indicate an origin deeper than normally tapped by a spreading center. White and McKenzie (1989, 1995) estimate that melting begins at depths of 110 km or greater and extends to depths of 70–30 km. Watson and McKenzie (1991) have carried out a detailed study of melt generation at Hawaii. They estimate that the maximum mantle adiabat has a potential temperature of 1,830 K, that the degree of partial melting is 6.9%, and that the depth range of melting is 127–72 km.

Chemical differences in basalts along the mid-ocean ridges also indicate excess temperature beneath hot spots. Klein and Langmuir (1987) used variations in crustal Na_2O content and its correlation with ridge crest topography to infer excess potential temperatures of about 250 K for ridge-centered hot spots. Schilling (1991) used variations in trace element concentrations along the mid-Atlantic ridge to infer excess potential temperatures near 200 K for Atlantic hot spots. High upwelling temperatures at hot spots in continental regions also suggest a deep source of melting. Crough et al. (1980) have argued that kimberlites, which are known to come from below 100 km depth, are associated with hot spot tracks on continental cratons.